Deciphering the Fluorescence Resonance Energy Transfer Signature of 3-Pyrazolyl 2-Pyrazoline in Transport Proteinous Environment

Paltu Banerjee, Smritimoy Pramanik, Arindam Sarkar, and Subhash Chandra Bhattacharya*

Department of Chemistry, Jadavpur University, Kolkata 700032, India

Received: December 30, 2008; Revised Manuscript Received: June 15, 2009

In the present investigation, an attempt has been made to study the interaction of newly synthesized bioactive compound 3-pyrazolyl 2-pyrazoline (PZ) with model transport proteins, bovine serum albumin (BSA), and human serum albumin (HSA) employing steady state and time-resolved fluorescence technique. We have focused on fluorescence resonance energy transfer (FRET) between excited tryptophan in transport proteins to transport-proteins-bound PZ. An efficient Förster-type resonance energy transfer from the tryptophan residues to PZ indicates that PZ binds in the vicinity of the tryptophan residue. Binding of protein to that bioactive compound without changing conformation of primary and secondary structure of protein has been monitored using circular dichroism (CD) study.

Introduction

Spectroscopic techniques for probing the structure, dynamics, and function of the biological system mainly based on fluorescence from the tryptophan residue buried within the core of the protein molecules have been of increasing great interest in applied fields. Serum albumins, rich in plasma, are the most widely studied proteins. Structural aspects and properties of these transport proteins have been well explored. These transport proteins of 580 amino acid residues are composed of a single polypeptide chain and are characterized by a high content of cystine, stabilizing a series of nine loops and a low content of tryptophan. These serum albumins consist of 67% of helix of six turns and 17 disulfide bridges in their secondary structures.[1] The tertiary structure is composed of three α-helical domains I−III. Each domain consists of two subdomains named as IA, IB, IIA, IIB, IIIA, and IIIB.[1,2] Bovine and human serum albumins (BSA and HSA) exhibit approximately 80% ordered homology and a repeating pattern of strictly conserved disulfide. The high affinity photosensitizer-binding sites on serum albumin have been classified into two well-exemplified groups, sites I and II, which are located in hydrophobic cavities in subdomains IIA and IIIA. As domain II and III share a common interface, binding a probe to domain III leads to conformational changes affecting the binding affinities to domain II. Despite the size and complexities of HSA, there is only a single tryptophan residue (Trp-214) in domain II which facilitates the study of protein from a spectroscopic point of view. In the case of BSA, there are two tryptophan residues (Trp 134 and Trp 212). Trp-212 is found localized in a similar hydrophobic microenvironment as single tryptophan residue of HSA but additional tryptophan residue (Trp-134) in BSA is found localized in the second helix of the first domain and is more exposed to solvent.[3]

Serum albumins have been branded as major protein constituents of blood plasma, which assist the disposition and transport of various exogenous and endogenous ligands to specific targets.[4] Bovine serum albumin (BSA) and human serum albumin (HSA) are frequently used in biophysical and biochemical studies. They also play an important role in drug disposition and efficacy. The unique feature of albumin is its ability to bind drug and other bioactive molecules[5,6] mainly because of the availability of hydrophobic pockets inside the protein network and the flexibility of the albumins in adapting their shapes. Serum albumins increase the solubility of hydrophobic drugs in plasma effectively and modulate those drugs delivery to the cells in vivo and vitro. Albumins are the principal biomacromolecules that are involved in the maintenance of colloid-blood pressure needed for proper distribution of body fluids between intravascular compartments and body tissues.[7] They also act as a plasma carrier by nonspecific binding through several hydrophobic steroid hormones across organ−circulatory interfaces such as the liver, intestine, kidney, and brain.[8]

Spectroscopic method has been extensively applied in investigating drug binding with albumin under physiological conditions because of its accuracy, sensitivity, rapidity, and convenience in handling.[9] Fluorescence resonance energy transfer (FRET) is a fluorescence phenomenon during which energy is transferred nonradiatively from one fluorescent molecule (donor) to a second fluorophore (acceptor).[10] It has been widely used to study the structure and dynamics of molecules in the gas phase, solution phase, and solid state.[10,11] Fluorescence resonance energy transfer is a powerful spectroscopic technique that allows biological relevant distances between 20 and 80 Å to be quantified under physiological conditions with near angstrom resolution due to the strong distance dependence of the transfer process. According to Förster, the excitation spectrum of the acceptor must overlap with the emission spectrum of the donor.[12] The radiative orientation of the transition dipoles of the participant also has an influence on the efficiency of energy transfer, and the FRET process is strongly dependent on the distance between the participants. According to Förster's theory the rate of energy transfer depends mainly upon the following factors:[12−15] (a) the extent of spectral overlap between the donor emission and the acceptor absorption spectra, (2) the quantum yield of the donor (Φ_f^D), (3) the relative orientation of the donor and acceptor transition dipoles, and (4) the distance between the donor and acceptor transition dipoles.

2-Pyrazoline derivatives constitute a class of compounds of pharmaceutical importance.[16−19] Recent trends to synthesize

* To whom correspondence should be addressed. E-mail: scbhattacharyya@chemistry.jdvu.ac.in. Tel.: 033 2414 6223. Fax: 91(033) 241465.

10.1021/jp811479r CCC: $40.75
Published on Web 07/27/2009

SCHEME 1: Structure of PZ

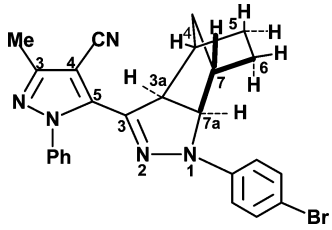

these types of compounds have been augmented for their anti-inflammatory, antidiabetic, anesthetic, analgesic, and glutamate transport sensor properties.[20−24] The interest on the interaction of pyrazoline derivatives with protein using FRET originates principally from two aspects−the first stems from its novel biological applications in pharmaceuticals and the second one arises due to the presence of electron donors and acceptors at N(1) and C(3) positions, respectively. These bioactive fluorescent molecules can effectively serve as reporters of the psychological activities in living systems.

The solvent dependent radiative transitions and relaxation dynamics of pyrazole substituted 2-pyrazoline (PZ) from S_1 and S_2 states have been established in our earlier publication.[25] In previous studies from our research laboratory, interesting uses of PZ as a sensitive fluorescence probe for exploring the local environments in membrane mimetic organized assemblies were demonstrated.[26]

The interactions between PZ and these biological receptors are yet to be investigated. In the present paper, the interaction of 2-pyrazoline derivatives with the high sensitive model transport protein has been studied using both steady state and time-resolved spectroscopy. The results have been analyzed from the spectroscopic viewpoint. The application of bioactive compound as a sensor of tryptophan residue has been demonstrated to be an effective approach for studying protein microenvironment and dynamics.

Experimental Section

3-Pyrazolyl-2-pyrazoline derivative, 5-((3a*S*,7a*R*)-1-(4-bromophenyl)-3a,4,5,6,7,7a-hexahydro-1*H*-4,7-methano-indazol-3-yl)-3-methyl-1-phenyl-1*H*-pyrazole-4-carbonitrile (Scheme 1) was synthesized using the method described earlier.[25]

The compound was further vacuum-sublimed before use. BSA (98%, fraction V, SRL) and HEPES (*N*-[2-hydroxyethyl]-piperazine-*N*′-[2-ethanesulphonicacid]) and HSA (Sigma, >96%) were used as received. A 50 mM buffer solution was prepared, and its pH was adjusted to 7.0. The same buffer solution was used as a medium throughout the experiment. Triply distilled water was used for the preparation of the experimental solutions. The purified solvents were found to be free from impurities and were transparent in the spectral region of interest.

Absorption spectra were recorded using a Shimadzu (Japan) UV−vis 1700 spectrophotometer with a matched pair of silica cuvettes. Fluorescence spectra were taken in a Fluorolog F-II A spectrofluorimeter (Spex Inc., NJ) with an external slit width of 1.25 mm. All measurements were done repeatedly, and reproducible results were obtained. All fluorescence spectra were corrected for the instrumental response.

Fluorescence lifetimes were determined from time-resolved intensity decay by the method of time-correlated single-photon counting using a nanosecond diode laser both at 403 nm (IBH, picoLED-07) and 295 nm (IBH, N-295) as light source. The typical response times of the laser system at 403 and 295 nm were 70 and 10 ps, respectively. The data stored in a multi-channel analyzer was routinely transferred to IBH DAS-6 decay analysis software. For all the lifetime measurements the fluorescence decay curves were analyzed by a biexponential iterative fitting program provided by IBH such as

$$F(t) = \sum_i \alpha_i \exp(-t/\tau_i) \tag{1}$$

where α_i is a pre-exponential factor representing fractional contribution to the time-resolved decay of the component with a lifetime τ_i. Mean (average) lifetimes $\langle\tau\rangle$ for biexponential decays of fluorescence were calculated from the decay times and pre-exponential factors using the following equation[27]

$$\langle\tau\rangle = \frac{\alpha_1\tau_1 + \alpha_2\tau_2}{\alpha_1 + \alpha_2} \tag{2}$$

Circular dichroism (CD) spectra were recorded on a JASCO J-720 spectropolarimeter, using a cylindrical cuvette with 1 mm path length. The CD profiles were obtained employing a scan speed of 20 nm/min and signal averaged for four successive scans. Appropriate baseline corrections in the CD spectra were made. For the CD experiment, BSA concentration was kept at 6 μmol dm^{-3}.

Results and Discussion

Emission Behavior of PZ in Protein. Figure 1A shows the emission spectra of PZ in the presence of different concentrations of BSA obtained on selective excitations of the probe at $\lambda_{exc} \approx 396$ nm. In absence of BSA, PZ emits very weakly giving rise to a green emission band at $\lambda_{em} \approx 496$ nm. Interestingly, on addition of protein (BSA), the emission profile shows dramatic changes leading to the appearance of a greatly blue-shifted emission band centered at ~486 nm accompanied by enhancement in the fluorescence emission intensity. In the case of HSA, a similar type of fluorescence like BSA has been observed but the band is centered at 476 nm. The observed blue shift in the emission maximum of PZ (from 496 nm in aqueous buffer to 486 nm in case of BSA and 476 nm in case of HSA) can be attributed to restriction on the solvent dipolar−dipolar relaxation imposed by the motionally constrained environment of the fluorophore in the protein matrix residing in the hydrophobic region. The increase in intensity further indicates that progressive binding of the probe to the protein makes nonradiative channels usually present in aqueous buffer medium less operative.[28]

The enhancement of fluorescence intensity of PZ in protein solution can be rationalized in terms of binding of the probe PZ with the protein. But the strength of the binding can be identified through the determination of the binding constant between the probe and the protein. The binding constants between the probe and the protein have been determined from the fluorescence intensity data following the method described by Almgren et al.[29]

According to this method

$$\frac{F_\infty - F_0}{F - F_0} = 1 + \frac{1}{K[\text{protein}]} \tag{3}$$

where, F_0, F, and F_∞ are the fluorescence intensities of PZ in the absence of protein, in protein solution, and under conditions

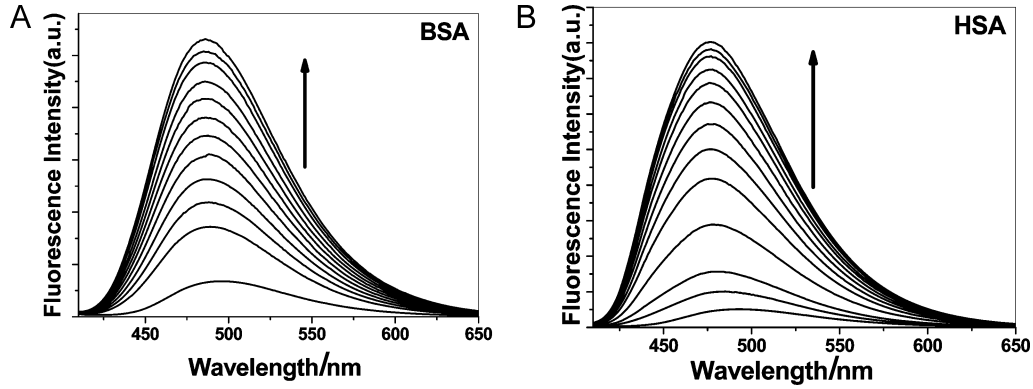

Figure 1. (A) Fluorescence spectra of PZ solution with increasing BSA concentrations (λ_{exc} = 396 nm); (B) fluorescence spectra of PZ solution with increasing HSA concentrations (λ_{exc} = 396 nm).

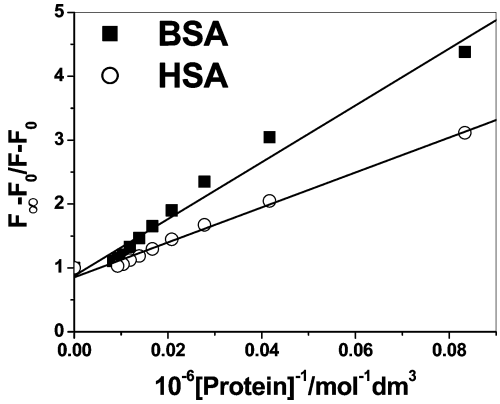

Figure 2. The plot of $(F_\infty - F_0)/(F - F_0)$ vs $[\text{protein}]^{-1}$ for the determination of binding constant. Protein: BSA (■), HSA (○).

of complete saturation of binding between probe and protein, respectively. K represents the binding constant between the probe in the excited state and protein.

The plot of $(F_\infty - F_0)/(F - F_0)$ vs 1/[protein] in relation to eq 3 shows the linearity [Figure 2]. The binding constant values are tabulated in Table 1. The determined K values (±10%) fall in the normal range reported previously for such type of complexations.[28,30,31] From a glance at the relative values of K (Table 1), it is evident that the probe binds in a stronger way with HSA as compared to BSA. This greater degree of association of the probe with HSA is reflected on the larger fluorescence enhancement with larger wavelength shift of the fluorophore in case of HSA with the addition of a definite amount of BSA or HSA.

Energy Transfer from Transport Proteins to PZ. FRET is a nondestructive spectroscopic method that can monitor the proximity and relative angular orientation of fluorophores and is ideal for the sensitive detection of the molecular binding events and changes in protein conformation in response to interaction with a particular target molecule.[32] Transfer of energy could take place through direct electrodynamic interaction between the primarily excited molecule (donor) and its neighbors (acceptors). The most widely spread application of this phenomenon is its use as "spectroscopic ruler".[10,33] The spectroscopic ruler is suitable for distance measurement in several nanometers.

Using FRET, the distance "r" between PZ and BSA or HSA (Trp-214) could be calculated by the equation.

$$E = 1 - \frac{F}{F_0} = \frac{{R_0}^6}{{R_0}^6 + r^6} \tag{4}$$

where, E denotes the efficiency of energy transfer between the donor and the acceptor, and R_0 (Förster radius), measured in Å unit, is the critical distance when the efficiency of transfer is 50%;[34] r is the distance between donor and acceptor.

$${R_0}^6 = 8.79 \times 10^{-25} \chi^2 n^{-4} \phi J \tag{5}$$

In eq 5, χ^2 is the orientation factor related to the geometry of the donor and acceptor of dipoles and $\chi^2 = {}^2/_3$ for random orientation as in fluid solution; n is the average refractive index of medium in the wavelength range where spectral overlap is significant; ϕ is the fluorescence quantum yield of the donor; J is the effect of the spectral overlap between the emission spectrum of the donor and the absorption spectrum of the acceptor (Figure 3), which can be calculated by the equation:

$$J = \frac{\int_0^\infty F(\lambda)\, \varepsilon(\lambda)\, \lambda^4\, \mathrm{d}\lambda}{\int_0^\infty F(\lambda)\, \mathrm{d}\lambda} \tag{6}$$

where, F(λ) is the corrected fluorescence intensity of the donor in the wavelength range from λ to $\lambda + \Delta\lambda$; $\varepsilon(\lambda)$ is the extinction coefficient of the acceptor at λ.

Figure 4A and 4B show change in fluorescence of BSA/HSA upon addition of PZ, the fluorescence intensity at 343 nm corresponding to decrease in albumin, whereas that at 496 nm of PZ increased and clear isoemissive points appeared at 432 and 415 nm for BSA and HSA, respectively. In our experiment, we found that determination of the FRET efficiency by measuring the decrease in the donor fluorescence is more reproducible than determination of the FRET efficiency based on increase in the acceptor fluorescence.

In our case, $\chi^2 = {}^2/_3$, $n = 1.36$, and $\phi = 0.15$, according to the eqs 4−6, calculated J values are 1.39×10^{-12} cm^3 L mol^{-1} and 1.56×10^{-12} cm^3 L mol^{-1} for BSA and HSA, respectively. The Förster radius (R_0) and the average distances (r) are tabulated in Table 1. The average distances between a donor fluorophore and acceptor fluorophore are on the 2−8 nm scale and $0.5R_0 < r < 1.5R_0$, which indicate that the energy transfer from transport proteins to PZ occurs with high probability.

Fluorescence Quenching. To confirm the quenching mechanism, we analyzed the fluorescence quenching data by the well-known Stern−Volmer equation. The bimolecular quenching rate

TABLE 1: Various Energy Transfer Parameters, Quenching Parameters and Binding Constant of PZ in Proteinous Environment

donors	Förster radius (R) (Å)	energy transfer efficiency (%)	distance between donor and acceptor (r) (Å)	Stern−Volmer constant ($K_{SV} \times 10^{-4}$) ($mol^{-1}dm^3$)	binding affinity ($K_A \times 10^{-4}$) ($mol^{-1}dm^3$)	binding sites (n)	binding constant ($K \times 10^{-4}$) ($mol^{-1}dm^3$)
BSA	56.0	11	82.7	1.39	1.33	1.34	2.24
HSA	57.2	25	71.3	3.62	4.37	0.9	3.65

constant (k_q) and Stern−Volmer quenching constant (K_{SV}) were obtained on the basis of the Stern−Volmer equation[10] as follows

$$\frac{F_0}{F} = 1 + K_{SV}[Q] = 1 + k_q\tau_0[Q] \qquad (7)$$

where F_0 and F denote the steady state fluorescence intensities of proteins in the absence and in the presence of quencher (PZ), respectively. K_{SV} is the Stern -Volmer quenching constant, and [Q] is the concentration of quencher; τ_0 is the average lifetime of the fluorophore in the absence of the quencher.

From the plot F_0/F vs [Q] (Figure 5), slope represents K_{SV}. The linearity of the plot indicates that only one type of quenching occurs in the systems.[10] In the presence of quencher the absorption spectra of the transport protein remain unaltered. This indicates that the static quenching does not occur. The Stern−Volmer quenching constant has been determined and the values are given in Table 1.

The quenching rate constants are of the order of 10^{12} s^{-1} which is higher than the maximum diffusion collision rate constant of various quenchers with the biopolymer (2.0×10^{10} L $mol^{-1}s^{-1}$). The higher K_{SV} or k_q values reveal the specific interaction between them. Since there is good overlap region between the fluorescence spectra of proteins and absorption spectra of the quencher, the fluorescence resonance energy transfer occurs during the quenching process.

Association of the probe with protein has been analyzed from the fluorescence quenching data. Analysis of the data was also performed via the method reported by Wang et al.[35] The tryptophan residue fluorescence intensity was scaled with the PZ concentration [PZ] through the relation in eq 8. The number of binding sites was obtained according to the eq 8[35] by plotting $\log((F_0 - F)/F)$ vs $\log [Q]$.

$$\log\left(\frac{F_0 - F}{F}\right) = \log K_A + n \log[Q] \qquad (8)$$

The slope of the double logarithm plot obtained from the experimental data was the number of equivalent binding sites (n).

The determined results showed that the number of binding sites was $n = 0.9 \pm 0.1$ for HSA and 1.34 ± 0.1 for BSA suggesting that one molecule of the protein combined with one molecule of that bioactive compound. For $n \approx 1$, eq 8 can be rewritten to the following eq 9. The binding affinities of the PZ with proteins can be obtained from the slopes of the

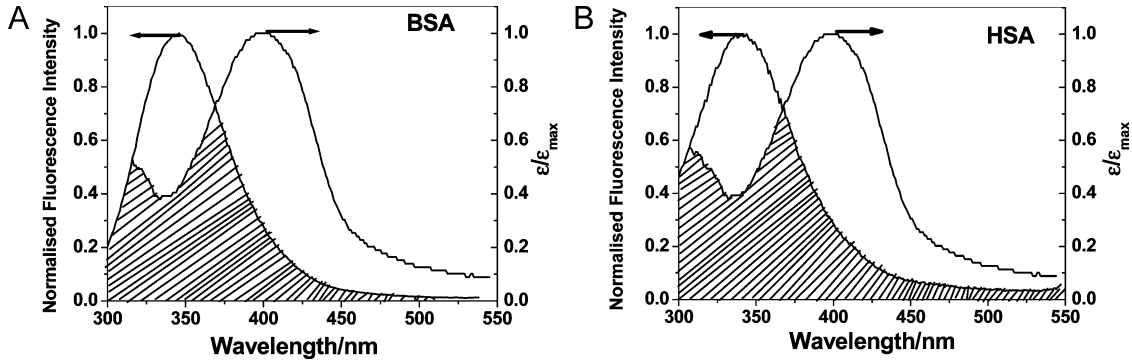

Figure 3. (A) The overlap of the normalized fluorescence spectra of donor BSA and the relative absorption spectra of acceptor PZ; (B) the overlap of the normalized fluorescence spectra of donor HSA and the relative absorption spectra of acceptor PZ.

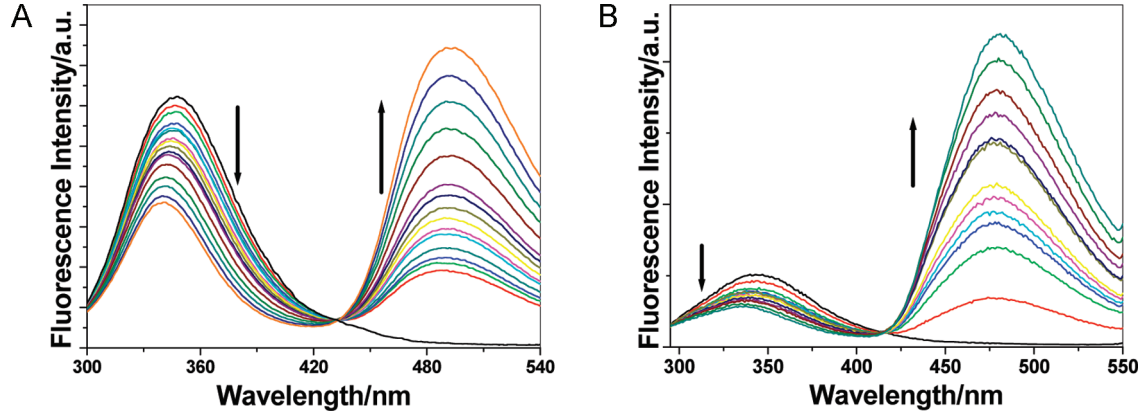

Figure 4. (A) Fluorescence resonance energy transfer profile from BSA to PZ; (B) fluorescence resonance energy transfer profile from HSA to PZ.

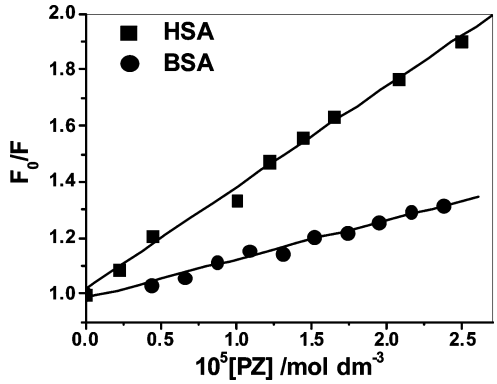

Figure 5. Plot of relative fluorescence intensity (F_0/F) vs [PZ]. Here PZ acts as a quencher.

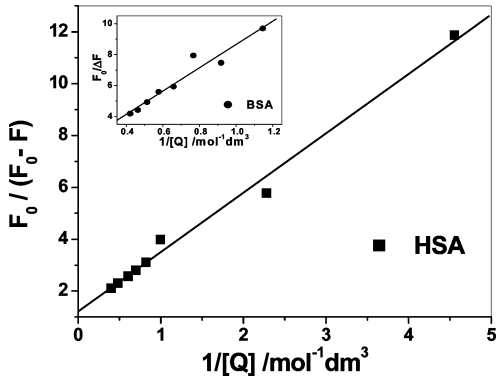

Figure 6. Plot of $F_0/(F_0 - F)$ vs 1/[Q] for HSA binding. (Inset) Same type of plot for BSA binding.

double reciprocal curves (Figure 6) of $F_0/(F_0 - F)$ vs $[Q]^{-1}$ and tabulated in Table 1.

$$\frac{F_0}{F_0 - F} = 1 + \frac{1}{K_A}\frac{1}{[Q]} \tag{9}$$

The binding affinity and binding constant value agree well with each other. From the value of binding constant and binding affinity (Table 1), it can be seen that the intensity of binding of HSA and PZ was greater than the one of BSA and PZ. It was probably due to the different constructions of HSA and BSA and different orientation toward the probe molecule.

Time Resolved Studies. Fluorescence lifetime serves as a sensitive indicator of the local environment in which a given fluorophore is placed.[36] Lifetime-based measurements are rich in information and provide unique insights into the systems under investigation.[37] In proteinous environment, there is a biexponential decay of PZ and the lifetime values are observed to be longer than those measured in aqueous buffer solution. The typical biexponential decay profiles of PZ in those environments are shown in Figure 7. The fluorescence lifetime of PZ in those environments are represented in Table 2.

Without putting emphasis on the magnitude of individual decay constants in such biexponential decays, we desire to use the mean fluorescence lifetime (Table 2) as a valuable parameter for exploiting the nature of the PZ molecule bound to protein.

We were also keen to study the fluorescence decay of protein (both BSA and HSA) at different molar ratios of the bioactive photosensitizer PZ to obtain a picture about the change in the microenvironment of that fluorophore upon binding to protein. Figure 8 represents the time-resolved decays of protein at pH

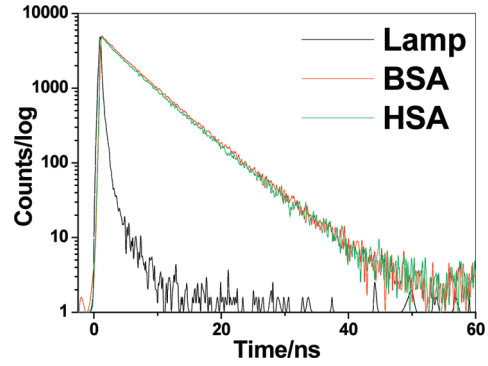

Figure 7. Typical fluorescence decay curves associated with lamp profile for PZ in proteinous environment. Curve is shown in biexponential fits. Excitation wavelength is kept at 403 nm.

TABLE 2: Fluorescence Lifetime of PZ in Buffer and Protein Environment

environment	α_1	τ_1/ns	α_2	τ_2/ns	τ_{av}/ns
buffer	0.48	0.70	0.52	2.38	1.57
BSA	0.13	2.97	0.87	6.11	5.70
HSA	0.05	2.29	0.95	5.94	5.75

7.02. Fluorescence lifetimes and their amplitudes are presented in Table 3. As tryptophan is known to exhibit multiexponential decays,[38] we have not attempted to assign the individual components. The origin of the multiexponential decays of the fluorescence from proteins is a puzzle toward many researchers. There are several possible origins: ground state heterogeneity, time-depended relaxation around the excited state or the intrinsic heterogeneity of tryptophan fluorescence. Although many researchers have reported three exponential decays of lifetime of tryptophan residue,[38,39] we have considered the biexponential decay, general trend of lifetimes of tryptophan residue based on appropriate residual and reduced χ^2 values. However, the average lifetimes of HSA/BSA have been used in order to gain a qualitative picture. It is familiar that the energy transfer depends on the lifetime of the donor molecule (eq 10).

$$k_T(r) = \frac{1}{\tau_D}\left(\frac{R_0}{r}\right)^6 \tag{10}$$

With gradual addition of a micromolar amount of an acceptor probe solution, the lifetime of the donor decreases (shown in Table 3 with Figure 8). Now we can calculate the rate constant of energy transfer ($k_T(r)$) by eq 10.

The values of k_T for BSA−PZ systems and HSA−PZ systems are 0.2×10^8 ns^{-1} and 0.6×10^8 ns^{-1}, respectively. The rate of energy transfer for HSA−PZ systems is three times higher than that of BSA−PZ systems. It may be rationalized from the viewpoint of intrinsic heterogeneity and time depended relaxation variation of different tryptophan residue of BSA and HSA. This finding also correlates with distinct energy transfer efficiency and binding constant.

The average lifetime decreases from 5.9 to 4.7 ns for BSA and 4.2 to 3.5 ns for HSA at maximum fluorophore concentration. This observation also correlates with our previous inferences obtained from steady-state experiment that its quenching is due to FRET by only effective binding of the fluorophore in the vicinity of tryptophan residue.

Kinetic Analysis of Decay Curves. As average lifetimes provide a qualitative picture, we have attempted to introduce a kinetic analysis considering only fractional contribution of the

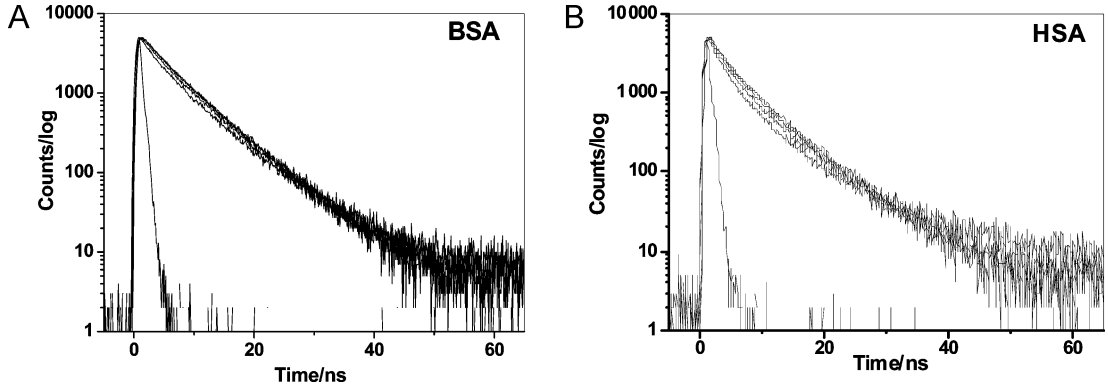

Figure 8. (A) Typical fluorescence decay curves associated with lamp profile for BSA in water, with variation of [PZ]. Curve is shown biexponential fits. Excitation wavelength is kept at 295 nm. (B) Typical fluorescence decay curves associated with lamp profile for HSA in water, with variation of [PZ]. Curve is shown biexponential fits. Excitation wavelength is kept at 295 nm.

individual lifetime component. We have obtained biexponential decays of the fluorescence of protein fluoprophore. Generally, a system that consists of fluorophores in different environments, or different kinds of fluorophores, will yield complex kinetic information because the fluorophores are likely to have different excited-state lifetimes and be subject to different decay process with different fractional contribution.[40] Analysis of the time-resolved fluorescence decay kinetics for such a system is not straightforward, specially without a priori knowledge of the appropriate kinetic model, because the analysis involves resolution of multiple, highly correlated kinetic parameters. First of all, we consider an equilibrium between tryptophan residue of HSA exposed toward its own domain and that exposed to solvent. When PZ is introduced into this environment, it also simultaneously distributed according to tryptophan orientation. Destabilizing the former equilibrium process, two new types of equilibrium processes arise through two different complexations. After short time complexation, both decay processes run. In the presence of PZ, whole protein has been converted to the complex. But the complexation ratio depends on increase of PZ concentration.

$$HSA_1 \rightleftharpoons HSA_2$$

$$HSA_1 + PZ \rightleftharpoons HSA_1\cdots PZ$$

$$HSA_2 + PZ \rightleftharpoons HSA_2\cdots PZ$$

So the equilibrium constant or here binding constant K can be represented as

$$K = \frac{[HSA_1\cdots PZ]}{[HSA_1][PZ]} \quad \text{or,} \quad \frac{[HSA_1\cdots PZ]}{[HSA_1]} = K[PZ] \qquad (11)$$

where [HSA···PZ] and [HSA_1] are the concentration of PZ-bounded one-type of HSA and the free type of HSA, that is, before complexation through energy transfer. A similar type of representation can be shown for another type of HSA. However, now in our case, fractional contribution obtained from time-resolved studies (Table 3) provide basically nothing but complexation concentration. We can plot the ratio of fractional contribution after complexation (α_1 or α_2) and before complexation (α_0) of donor and acceptor with the variation of acceptor concentration [PZ] as acceptor resembling that with quencher.

From the curves, it seems that the quantum yield of [HSA_1···PZ] is less than that of [HSA_2···PZ]. The binding

TABLE 3: Fluorescence Lifetime of HSA and BSA as a Function of Concentration of PZ

[PZ] (μm)	α_1	τ_1 (ns)	α_2	τ_2 (ns)	τ_{av} (ns)	χ^2
			HSA			
0	0.65	2.33	0.35	7.67	4.20	1.00
0.8	0.57	2.31	0.43	6.64	4.17	1.10
1.6	0.62	2.29	0.38	6.79	4.00	1.10
2.4	0.63	2.14	0.37	6.52	3.76	1.07
3.2	0.67	2.14	0.33	6.53	3.58	1.12
5.2	0.72	2.18	0.28	6.80	3.47	1.15
			BSA			
0	0.52	4.35	0.48	7.48	5.85	1.07
0.9	0.42	3.70	0.58	7.08	5.66	1.08
1.6	0.45	3.40	0.55	7.03	5.40	1.20
2.4	0.38	2.96	0.62	6.85	5.37	1.11
3.2	0.31	2.06	0.69	6.52	5.14	1.14
5.2	0.43	2.80	0.57	6.84	5.09	1.18
9.1	0.55	2.78	0.45	7.02	4.69	1.14

constant values obtained from HSA···PZ complexation are 5.1×10^4 and 9.8×10^4 mol^{-1} dm^3 for types 1 and 2, respectively. In the case of BSA, two types of linearity (second part of linearity shown in Figure 9) provide same order of results: 1.2×10^4 and 6.2×10^4 mol^{-1} dm^3 for types 1 and 2, respectively. It can be rationalized that the same type of residue Trp-214 for HSA and Trp-212 for BSA provide similar observation. The question arises now, what is responsible for first part of diverse linearity in both BSA_1 and BSA_2? It may be due to additional tryptophan residue Trp-134 in BSA, which is found localized in the second helix of the first domain and is more exposed to solvents. Additional experimental protocol may be required to resolve this problem, and this would be our future work.

Structural Stability of Transport Protein. To detect the possible influence of biocompound PZ binding on the secondary structures of BSA and HSA, we have performed far UV circular dichroism in both albumin proteins in the absence and presence of the PZ. Consistent with the literature, the CD spectra for the BSA and HSA solutions, monitored in the range 250−200 nm, showed two bands at 209 and 222 nm.[41] Figure 10 represents a set of representative CD spectra for the BSA-PZ system. The superimposed CD spectra of the proteins in the absence and presence of the probe reveal that, at least in the experimental concentrations range, there is no perceptible structural change of the proteins upon binding with the probe. Chakrabarty et al.[38] had reported a similar type of observation earlier. Besides this, it also needs to be said that there was no appreciable change in the primary structure of probe in the presence of protein when the CD spectra was monitored in the range 350−450 nm (figure not shown here).

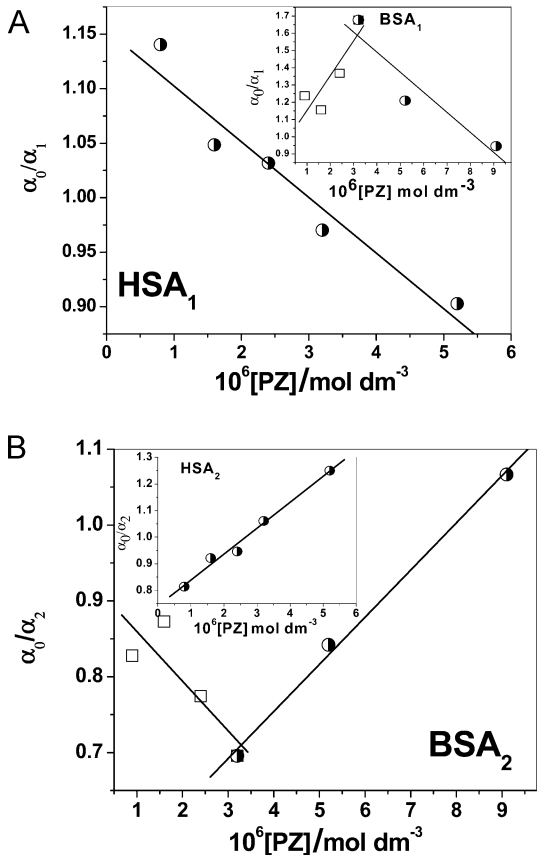

Figure 9. (A) Ratiometric plot of fractional contribution for HSA_1 and BSA_1 with varying concentration of PZ. (B) Ratiometric plot of fractional contribution for HSA_2 and BSA_2 with varying concentration of PZ.

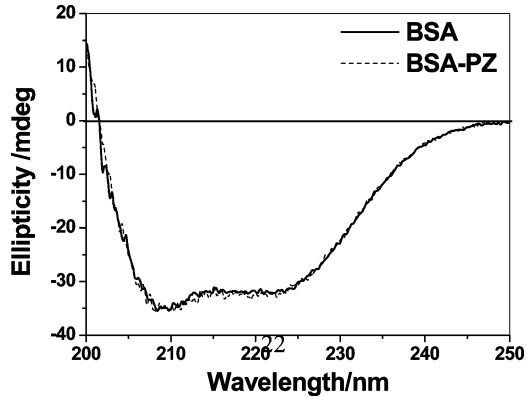

Figure 10. CD spectra of BSA in the absence and presence of PZ from 200 to 250 nm.

Conclusions

The research described herein provides insights into the photophysical properties of PZ in a typical protein environment. We have demonstrated enhancement of the sensitized acceptor emission from one binding event by utilizing a potentially bioactive compound PZ along with upconverting model transport proteins (BSA and HSA) as energy donor. The binding constants of the protein with the probe have been estimated and the high order of values implies fluorescence resonance energy transfer from the donor to the acceptor. The binding stoicheomety *n* of PZ to proteins has been calculated. It has been found that the intensity of binding between PZ and HSA is greater than the one of binding between BSA and PZ. Kinetic analysis of decay curves provides kinetic information on donor−acceptor complexation. It can be expected that the fluorescence quenching technique could provide a promising tool to study the interaction of the fluorescent probe with proteins. This study will open up new avenues for the labeling of damaged proteins through their interaction with bioactive compounds.

Acknowledgment. This study was supported by CSIR (01(2057)/06/EMR-II), New Delhi funding agency. The authors are thankful for technological support from Professor S. Basak of SINP, Kolkata, in CD measurement. The authors are indebted to Prof. K. K. Mahalanabis and Dr. A. Mukherjee, Jadavpur University for their co-operation with the synthesis of the compound. The authors are also thankful to Prof. S.C. Bera, Jadavpur University, and Dr. A. Mallick of Kashipur M. M. Mahavidyalaya for their valuable discussion.

References and Notes

(1) Peters, T. *Serum Albumin. Advances in Protein Chemistry*; Academic Press: New York, 1985; p 161.
(2) Min, H. X.; Carter, D. C. *Nature* **1992**, *358*, 209.
(3) Peters, T. *Adv. Protein Chem.* **1985**, *37*, 161.
(4) (a) Peters, T. *All about Albumin: Biochemistry, Genetics and Medicinal Applications*; Academic Press: San Diego, CA, 1996. (b) Kumar, C. V.; Buranaprapuk, A. S. *Angew. Chem., Int. Ed. Engl.* **1997**, *36*, 2085.
(5) Kragh-Hansen, U. *Biochem. J.* **1985**, *225*, 629.
(6) Hu, Y.; Liu, Y.; Jiang, W.; Zhao, R.; Qu, S. *J. Photochem. Photobiol. B* **2005**, *80*, 235.
(7) Singer, S. J.; Nicolson, G. L. *Science* **1972**, *175*, 720.
(8) Partridge, W. M. *Am. J. Physiol.* **1987**, *252*, 157.
(9) Kamat, B. P.; Seetharamappa, J. *J. Chem. Sci.* **2005**, *117*, 649.
(10) Lakowicz, J. R. *Principles of Fluorescence Spectroscopy*, Kluwer Academic: New York, 1999.
(11) Selvin, P. R. *Nat. Struct. Biol.* **2000**, *7*, 730.
(12) Förster, Th. *Ann. Phys.* **1948**, *2*, 55.
(13) Turro, N. J. *Modern Molecular Photochemistry*; Benjamin/Cummings: Menlo Park, CA, 1978.
(14) Rohatgi-Mukherjee, K. K. *Fundamentals of Photochemistry*; Wiley Eastern: New Delhi, India, 1986.
(15) Sahoo, H.; Roccatano, D.; Zacharias, M.; Nau, W. M. *J. Am. Chem. Soc.* **2006**, *128*, 8118.
(16) Roelf Van, S. G.; Arnold, C.; Wellnga, K. *J. Agric. Food Chem.* **1979**, *84*, 406.
(17) Goodell, J. R.; Puig-Basagoiti, F.; Forshey, B. M.; Shi, P.-Y.; Ferguson, D. M. *J. Med. Chem.* **2006**, *49*, 2127.
(18) Kedar, R. M.; Vidhale, N. N.; Chincholkar, M. M. *Orient. J. Chem.* **1997**, *13*, 143.
(19) Singh, A.; Rathod, S.; Berad, B. N.; Patil, S. D.; Dosh, A. G. *Orient. J. Chem.* **2000**, *16*, 315.
(20) Garge, H. G.; Chandraprakash, J. *J. Pharm. Sci.* **1971**, *14*, 649.
(21) Krishna, R.; Pande, B. R.; Bharthwal, S. P.; Parmar, S. S. *Eur. J. Med. Chem.* **1980**, *15*, 567.
(22) Kucukguzel, S. G.; Rollas, S. *Farmaco* **2002**, *57*, 583.
(23) Jeong, T.-S.; Kim, K. S.; An, S.-J.; Cho, K.-H.; Lee, S.; Lee, W. S. *Bioorg. Med. Chem. Lett.* **2004**, *14*, 2715.
(24) Nakagawa, T.; Fujio, M.; Ozawa, T.; Minami, M.; Satoh, M. *Behav. Brain Res.* **2005**, *156*, 233.
(25) Chatterjee, S.; Banerjee, P.; Pramanik, S.; Mukherjee, A.; Mahalanabis, K. K.; Bhattacharya, S. C. *Chem. Phys. Lett.* **2007**, *440*, 313.
(26) Banerjee, P.; Pramanik, S.; Sarkar, A.; Bhattacharya, S. C. *J. Phys. Chem. B* **2008**, *112*, 7211.
(27) Shannigrahi, M.; Bagchi, S. *J. Photochem. Photobiol. A: Chem.* **2004**, *168*, 133.
(28) Mallick, A.; Haldar, B.; Chattopadhyay, N. *J. Phys. Chem. B* **2005**, *109*, 14683.
(29) Almgren, M.; Grieser, F.; Thomas, J. K. *J. Am. Chem. Soc.* **1979**, *101*, 279.
(30) Feng, X. Z.; Lin, Z.; Yang, L. J.; Wang, C.; Bai, C. *Talanta* **1998**, *47*, 1223.
(31) Pal, B.; Bajpai, P. K.; Basu Baul, T. S. *Spectrochim. Acta A* **2000**, *56*, 2453.
(32) Iqbal, S. S.; Mayo, M. W.; Bruno, J. G.; Bronk, B. V.; Batt, C. A.; Chambers, J. P. *Biosens. Bioelectron.* **2000**, *15*, 549.
(33) Stryer, L. *Annu. Rev. Biochem.* **1978**, *47*, 819.
(34) Sarkar, L. A.; Hudson, B. S.; Simoni, R. D. *Biochem.* **1977**, *16*, 5100.
(35) Kang, J.; Liu, Y.; Xie, M. X.; Li, S.; Jiang, M.; Wang, Y. D. *Biochim. Biophys. Acta* **2004**, *1674*, 205.

(36) Maciejewski, A.; Demmer, D. R.; James, D. R.; Safarzadeh-Amiri, A.; Verrall, R. E.; Steer, R. P. *J. Am. Chem. Soc.* **1985**, *107*, 2831.
(37) Bright, F. V.; Munson, C. A. *Anal. Chim. Acta* **2003**, *500*, 71.
(38) Chakrabarty, A.; Mallick, A.; Haldar, B.; Das, P.; Chattopadhyay, N. *Biomacromolecule* **2007**, *8*, 920.
(39) Grinvald, A.; Steinberg, I. Z. *Anal. Biochem.* **1974**, *59*, 583.
(40) Vyleta, N. P.; Coley, A. L.; Laws, W. R. *J. Phys. Chem. A* **2004**, *108*, 5156.
(41) Ahmad, B.; Parveen, S.; Khan, R. H. *Biomacromolecules* **2006**, *7*, 1350.

JP811479R